Reliable LIF/Mie droplet sizing in sprays using structured laser illumination planar imaging

Mishra, Yogeshwar; Kristensson, Elias; Berrocal, Edouard

Published in:
Optics Express

DOI:
10.1364/OE.22.004480

2014

Document Version:
Publisher's PDF, also known as Version of record

Reliable LIF/Mie droplet sizing in sprays using structured laser illumination planar imaging

Yogeshwar Nath Mishra, Elias Kristensson, and Edouard Berrocal*

Division of Combustion Physics, Department of Physics, Lund University, Box 118, Lund 22100, Sweden
edouard.berrocal@forbrf.lth.se

Abstract: In this article, Structured Laser Illumination Planar Imaging (SLIPI) is used in combination with the LIF/Mie ratio technique for extracting a reliable two-dimensional mapping of the droplets Sauter Mean Diameter (SMD). We show that even for the case of a fairly dilute spray, where single scattering events are in majority, the conventional LIF/Mie technique still remains largely affected by errors introduced by multiple light scattering. To remove this unwanted light intensity on both the LIF and Mie images SLIPI is used prior to apply the image ratio. For the first time, the SLIPI LIF/Mie results are calibrated and compared with measurement data from Phase Doppler Interferometry (PDI).

OCIS codes: (110.0113) Imaging through turbid media; (300.2530) Fluorescence, laser-induced; (290.5850) Scattering, particles; (290.4210) Multiple scattering.

References and links

1. N. Chigier, "An assessment of spray technology-editorial," Atomization Sprays **3**(4), 365–371 (1993).
2. W. D. Bachalo and M. J. Houser, "Phase Doppler spray analyzer for simultaneous measurements of drop size and velocity distributions," Opt. Eng. **23**(5), 583–590 (1984).
3. N. Roth, K. Anders, and A. Frohn, "Simultaneous measurement of temperature and size of droplets in the micrometer range," J. Laser Appl. **2**(1), 37–42 (1990).
4. R. A. Dobbins, L. Crocco, and I. Glassmans, "Measurement of mean particle sizes of sprays from diffractively scattered light," AIAA J. **1**(8), 1882–1886 (1963).
5. J. T. Kashdan, J. S. Shrimpton, and A. Whybrew, "A digital image analysis technique for quantitative characterisation of high-speed sprays," Opt. Lasers Eng. **45**(1), 106–115 (2007).
6. T. Shoba, C. Crua, M. Heikal, and M. Gold, "Optical characterisation of diesel, RME and kerosene sprays by microscopic imaging," in *24th European Conference on Liquid Atomization and Spray Systems (ILASS)* (Portugal, 2011).
7. C. N. Yeh, H. Kosaka, and T. Kamimoto, "A fluorescence/scattering imaging technique for instantaneous 2-D measurements of particle size distribution in a transient spray," in *Proceedings of the 3rd Congress on Optical Particle Sizing* (Japan, 1993), pp. 355–361.
8. T. Kamimoto, "Diagnostics of transient sprays by means of laser sheet techniques," in *International Symposium COMODIA* 94, pp. 33–41 (1994).
9. S. V. Sankar, K. E. Maher, D. M. Robart, and W. D. Bachalo, "Rapid characterization of fuel atomizers using an optical patternator," J. Eng. Gas Turbines Power **121**(3), 409–414 (1999).
10. P. Le Gal, N. Farrugia, and D. A. Greenhalgh, "Laser sheet dropsizing of dense sprays," Opt. Laser Technol. **31**(1), 75–83 (1999).
11. R. Domann and Y. Hardalupas, "Quantitative measurement of planar droplet sauter mean diameter in sprays using Planar droplet sizing," Part. Part. Syst. Charact. **20**(3), 209–218 (2003).
12. M. C. Jermy and D. A. Greenhalgh, "Planar dropsizing by elastic and fluorescence scattering in sprays too dense for phase Doppler measurement," Appl. Phys. B **71**(5), 703–710 (2000).
13. B. D. Stojkovic and V. Sick, "Evolution and impingement of an automotive fuel spray investigated with simultaneous Mie/LIF techniques," Appl. Phys. B **73**(1), 75–83 (2001).
14. S. Park, H. Cho, I. Yoon, and K. Min, "Measurement of droplet size distribution of gasoline direct injection spray by droplet generator and planar image technique," Meas. Sci. Technol. **13**(6), 859–864 (2002).
15. R. Domann and Y. Hardalupas, "A study of parameters that influence the accuracy of the planar droplet sizing (PDS) technique," Part. Part. Syst. Charact. **18**(1), 3–11 (2001).
16. G. Charalampous and Y. Hardalupas, "Numerical evaluation of droplet sizing based on the ratio of fluorescent and scattered light intensities (LIF/Mie technique)," Appl. Opt. **50**(9), 1197–1209 (2011).

#204922 - $15.00 USD Received 16 Jan 2014; revised 12 Feb 2014; accepted 13 Feb 2014; published 19 Feb 2014

17. G. Charalampous and Y. Hardalupas, "Method to reduce errors of droplet sizing based on the ratio of fluorescent and scattered light intensities (laser-induced fluorescence/Mie technique)," Appl. Opt. **50**(20), 3622–3637 (2011).
18. W. Zeng, M. Xu, Y. Zhang, and Z. Wang, "Laser sheet dropsizing of evaporating sprays using simultaneous LIEF/Mie techniques," Proc. Combust. Inst. **34**(1), 1677–1685 (2013).
19. A. Malarski, B. Schürer, I. Schmitz, L. Zigan, A. Flügel, and A. Leipertz, "Laser sheet dropsizing based on two-dimensional Raman and Mie scattering," Appl. Opt. **48**(10), 1853–1860 (2009).
20. D. L. Hofeldt, "Full-field measurements of particle size distributions. II: Experimental comparison of the polarization ratio and scattered intensity methods," Appl. Opt. **32**(36), 7559–7567 (1993).
21. S. Bareiss, B. Bork, S. Bakic, C. Tropea, R. Irsig, J. Tiggesbaumker, and A. Dreizler, "Application of femtosecond lasers to the polarization ratio technique for droplet sizing," Meas. Sci. Technol. **24**(2), 025203 (2013).
22. E. Kristensson, Structured Laser Illumination Planar Imaging: Applications for spray diagnostics (Ph.D. Thesis, Lund University, 2012).
23. E. Berrocal, I. Meglinski, and M. Jermy, "New model for light propagation in highly inhomogeneous polydisperse turbid media with applications in spray diagnostics," Opt. Express **13**(23), 9181–9195 (2005).
24. D. Stepowski, O. Werquin, C. Roze, and T. Girasole, "Account for extinction and multiple scattering in planar droplet sizing of dense sprays," in *13th International Symposium of Laser Techniques to Fluids Mechanics* (Lisbon, 2006), paper 1061.
25. E. Berrocal, E. Kristensson, M. Richter, M. Linne, and M. Aldén, "Application of structured illumination for multiple scattering suppression in planar laser imaging of dense sprays," Opt. Express **16**(22), 17870–17881 (2008).
26. E. Kristensson, E. Berrocal, M. Richter, and M. Alden, "Nanosecond structured laser illumination planar imaging for single-shot imaging of dense sprays," Atomization Sprays **20**(4), 337–343 (2010).
27. E. Berrocal, E. Kristensson, P. Hottenbach, M. Aldén, and G. Grünefeld, "Quantitative imaging of a non-combusting Diesel spray using structured laser illumination planar imaging," Appl. Phys. B **109**(4), 683–694 (2012).
28. E. Kristensson, L. Araneo, E. Berrocal, J. Manin, M. Richter, M. Aldén, and M. Linne, "Analysis of multiple scattering suppression using structured laser illumination planar imaging in scattering and fluorescing media," Opt. Express **19**(14), 13647–13663 (2011).
29. M. A. A. Neil, R. Juskaitis, and T. Wilson, "Method of obtaining optical sectioning by using structured light in a conventional microscope," Opt. Lett. **22**(24), 1905–1907 (1997).
30. D. J. Cuccia, F. Bevilacqua, A. J. Durkin, and B. J. Tromberg, "Modulated imaging: quantitative analysis and tomography of turbid media in the spatial-frequency domain," Opt. Lett. **30**(11), 1354–1356 (2005).

1. Introduction

Droplet size is one of the most important quantities of spray characteristics. The suitability of atomizing sprays for a variety of applications depends on the droplet size distribution over the full spray structure. For example, in medicine monodisperse droplets smaller than 5 μm are used for inhalation while polydisperse fuel droplets in the range of 5-20 μm are generated for combustion engineering purposes [1]. Industrial sprays require also a specific droplet size range depending on the needed process such as, cooling, painting, drying, applying chemical, dispersing liquids *etc*. It is therefore important to accurately measure droplet size distribution in sprays, preferably with both high spatial and temporal resolution.

In comparison to other existing techniques, the use of laser sheet imaging for droplet sizing is particularly advantageous: First, it is not a point measurement technique like Phase Doppler Interferometry (PDI) [2] or rainbow refractometry [3], second, it is not a line-of-sight approach like laser diffraction [4] or shadow imaging [5] and third, it is not restricted to a small field-of-view like high resolution microscopic imaging [6]. Laser sheet droplet sizing is thus very attractive because of its ability to directly provide a full-field measurement of a spray section. In the year 1993, the laser sheet based LIF/Mie ratio approach was first proposed for the characterization of a transient fuel spray [7]. Since then, the technique has been applied for a wide range of sprays such as in Diesel sprays in rapid compression engines [7,8], steady hollow-cone sprays for applications in gas-turbines or industrial burners [9–11], dense cooling sprays [12] and gasoline fuel injection systems [13,14]. In addition, some fundamental studies have been performed to evaluate the accuracy of the technique and its limitations [15–17]. In each of these articles, independent names of the LIF/Mie ratio technique have been given such as optical patternator [9], Laser Sheet Drop-sizing (LSD) [10] or Planar Droplet Sizing (PDS) [11]. In this paper we will refer to it as PDS.

#204922 - $15.00 USD Received 16 Jan 2014; revised 12 Feb 2014; accepted 13 Feb 2014; published 19 Feb 2014

The principle of PDS is based on the assumption that the LIF and Mie signals emerging from an ensemble of dye-doped droplets are proportional to their volume and surface area respectively. Planar images of these two signals are simultaneously recorded using, usually, two cameras of similar characteristics. Consequently, a pixel by pixel division of the LIF and Mie intensities can provide the droplets Sauter Mean Diameter (SMD or D_{32}) after careful calibration. It is assumed in PDS that the LIF signal is emerging from the droplets only and not from the surrounding medium. However, for highly evaporating sprays, the LIF signal originates from both the liquid and the gas phase, making the volumetric dependence of the LIF signal questionable. To overcome this issue, an Exciplex-based LIF scheme has been recently proposed and applied on a flash-evaporating spray [18]. To avoid the use of fluorescence tracers, two alternative schemes have been considered; one based on the ratio of Raman and Mie signals giving also D_{32} [19], and the other based on ratioing the vertical and horizontal polarization components of the scattered light, giving the droplets surface mean diameter (D_{21}) [20]. While Raman/Mie ratio is a good alternative to the LIF/Mie ratio, its applicability is restricted due to weak Raman signal leading to a low signal-to-noise (SNR) ratio. In the case of the Polarization Ratio (PR), the method is limited by errors induced by the strong oscillations from the Mie scattered light intensity. Recently, a femtosecond PR approach has been suggested to minimize these intensity oscillations [21]. The authors show that the use of 220 fs reduces the standard deviation of these oscillations from 30% to 9%, improving the precision of PR for sizing droplets between 25 μm and 200 μm. Nevertheless, shorter light pulses are required for accurately sizing droplets smaller than 25 μm.

Even though laser sheet based techniques possess attractive features, as previously mentioned, all of them easily suffer from issues related to the detection of multiple light scattering and yield non-reliable information. Thus, the measurement is rapidly restricted especially in optically dense sprays where the optical depth is larger than two (for a definition of optical depth, see pages 20-21 of reference [22]). To understand these effects Monte-Carlo (MC) simulations have been developed and applied. For example, Berrocal *et al.* have demonstrated, for the case of a hollow-cone spray, that the majority of the total number of detected photons are multiply scattered in laser sheet Mie imaging [23]. Another work [24] has shown that the light intensity from multiply scattered photons was prominent in planar Mie images of an air-blast atomizer. These investigations have contributed to the further understanding of light propagation through spray systems, and have led to the conclusion that multiple light scattering effects cannot be ignored.

The consequences of such effects were, however, not fully realized until the apparition in 2008 of Structured Laser Planar Illumination Imaging (SLIPI) [25, 26]. Recent results of the SLIPI in combination with PDS [27] have demonstrated that the multiple light scattering contributions are not the same in the recorded LIF and Mie signals and cannot, therefore, be cancelled by simply ratioing the two. It was shown that the undesired intensity must be first suppressed on both the LIF and Mie signals for reliable mapping of the relative SMD in a non-combusting Diesel spray. In addition, the results from an earlier publication which examines the accuracy, precision and limitations of SLIPI in scattering and fluorescing media have also supported its use for SMD mapping [28]. The novelty of the present article is to use the SLIPI LIF/Mie technique for a dilute hollow-cone water spray (of optical depth ~1 only) and to compare if the use of SLIPI is, in this case, still necessary or not. In addition, the results are calibrated and compared with results from PDI measurements in order to obtain, for the first time, a two-dimensional mapping of the absolute droplets SMD using SLIPI.

2. Description of the imaging techniques

2.1 SLIPI

SLIPI is an imaging technique combining structured illumination [29] with planar laser imaging. A Ronchi grating is usually used to imprint a modulated pattern along the vertical

#204922 - $15.00 USD Received 16 Jan 2014; revised 12 Feb 2014; accepted 13 Feb 2014; published 19 Feb 2014

direction of the light sheet. This special characteristic serves as a signature to tag the singly scattered photons from the illuminated plane. While those photons do "remember" the modulated signature, the multiply scattered photons will "forget" it rapidly while crossing a scattering medium like a spray system. Thus, the undisturbed modulated component, referred in the literature to as the *AC* component [30], becomes a faithful representation of the single light scattering. On the opposite, the contribution of the multiple light scattering mostly contains a non-modulated signature. The extraction of the single light scattering consists, then, in measuring the amplitude of the modulation. Due to the inhomogeneous nature of a spray system, this operation must be performed without deteriorating the spatial resolution of the image. If the light intensity structure imprinted on the light sheet is a sinusoidal, the resulting image intensity $I(x,y)$ is described as:

$$I(x,y) = I_C(x,y) + I_S(x,y)\cdot\sin(2\pi x\nu + \phi) \tag{1}$$

where ν represents the modulation frequency and ϕ is the spatial phase. Here, $I_C(x,y)$ is the intensity corresponding to singly and multiply scattered photons (*DC* component) and $I_S(x,y)$ represents the amplitude of the modulation from the singly scattered photons only (*AC* component). To experimentally extract the information corresponding to $I_S(x,y)$ in Eq. (1), a minimum of three intensity modulated images are recorded with a spatial phase corresponding to $0°, 120°$, and $240°$. With this recorded data, a SLIPI image can be constructed by extracting the root-mean square of the modulated images, described mathematically as:

$$I_S = \frac{\sqrt{2}}{3}\cdot\left[(I_0 - I_{120})^2 + (I_0 - I_{240})^2 + (I_{120} - I_{240})^2\right]^{1/2} \tag{2}$$

Similarly, a conventional image preserving both the multiply and singly scattered photons can be constructed by extracting the average of the three modulated images as:

$$I_C = \frac{I_0 + I_{120} + I_{240}}{3} \tag{3}$$

A complete and detailed description of the SLIPI technique can be found in Ref [22].

2.2 LIF/Mie droplet sizing

The SMD of spray droplets can be measured from the ratio of a signal proportional to the droplet volume, such as the fluorescence from the liquid phase, S_{LIF}, and a signal proportional to droplets surface area, such as the Mie scattered light, S_{Mie}. In addition, three conditions are required for the PDS technique to work: First, the spray droplets must be spherical. Second, the spray evaporation rate must be sufficiently slow to avoid fluorescence from the gas phase. Third, all photons reaching the camera should have experienced only one scattering event prior to detection. If those conditions are respected, the SMD of an ensemble of droplets, for each camera pixel, is equal to:

$$\mathrm{SMD} = \frac{\sum_0^\infty D_i^3}{\sum_0^\infty D_i^2} = \frac{\mathrm{S_{LIF}}}{\mathrm{S_{Mie}}}\cdot\frac{\mathrm{K_{LIF}}}{\mathrm{K_{Mie}}} \tag{4}$$

where K_{LIF} and K_{Mie} includes experimental components such as detector response, signal collection angle, laser power and dye concentration. There have been several experimental and theoretical studies [11, 15–17] focusing on the accuracy of the PDS technique. It was found that the ratio of K_{LIF}/K_{Mie} should not be considered as a constant, especially at

#204922 - $15.00 USD Received 16 Jan 2014; revised 12 Feb 2014; accepted 13 Feb 2014; published 19 Feb 2014

90° detection angle [16] as it has been assumed in earlier articles [7–10]. The real refractive index, scattering angle and dye concentration are parameters that strongly affect the relationship between scattered light intensity and droplets surface area. It is shown in [16] that the oscillations of the scattered light intensity are particularly large around 90° detection angle, while at 60°, the increase of the scattered light intensity in relation with the droplet diameter is smooth. The effect of multiple light scattering on PDS measurements has been demonstrated in [27] both for the case of a cuvette containing a homogeneous dispersion of polystyrene spheres and for a diesel spray at late time after injection start (between 2 ms and 3 ms). The results concluded that even a measure of the relative SMD (non-calibrated LIF/Mie ratio) were not acceptable if SLIPI was not used.

3. Description of the experiment

3.1 SLIPI LIF/Mie set-up

A steady state (continuously running) hollow-cone water spray of 60° spray angle is created using a pressure swirl nozzle of 1mm orifice diameter (Lechler, ordering no. 216.324). The spray is investigated at room temperature and atmospheric pressure conditions. The injection pressure is fixed at 20 bars producing a liquid flow rate of 1.26 liter/min. The injected water is seeded with a translucent fluorescing dye (Pyranine: Solvent green 7) from yellow highlighter's ink. The main reasons of choosing the yellow highlighter's ink as tracer are the non-toxicity and the high quantum efficiency of the dye when excited at $\lambda = 448$ nm. A top view schematic of the SLIPI setup used in this experiment is shown in Fig. 1. The center of the spray is illuminated (using a 448 nm collimated continuous wave diode laser) with a vertically modulated laser sheet of 5.8 cm in height. The broad-band LIF signal is peaking at 517 nm and the 448 nm narrow-band Mie signal are spectrally separated using a long pass

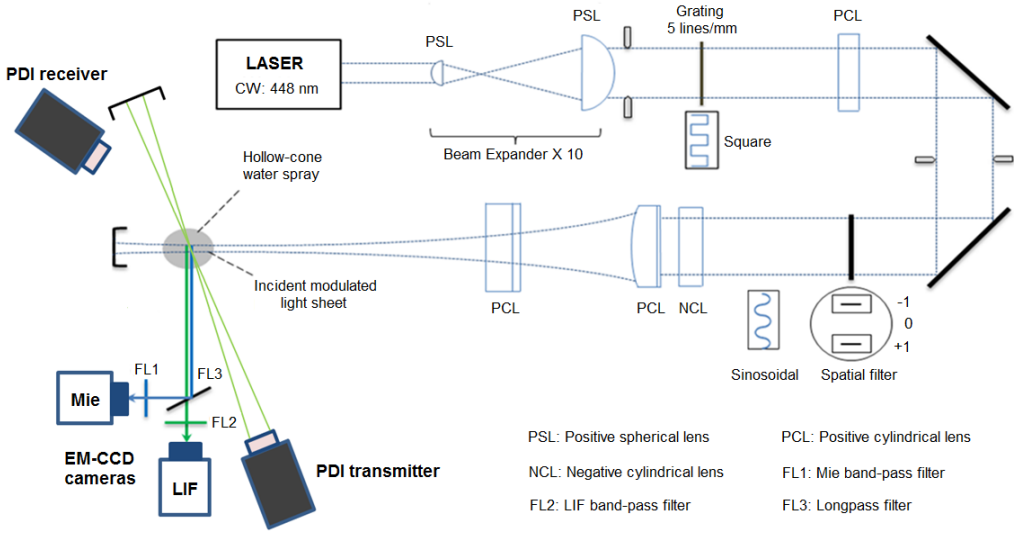

Fig. 1. Top-view of the SLIPI-LIF/Mie optical arrangement, together with the PDI set-up.

#204922 - $15.00 USD Received 16 Jan 2014; revised 12 Feb 2014; accepted 13 Feb 2014; published 19 Feb 2014

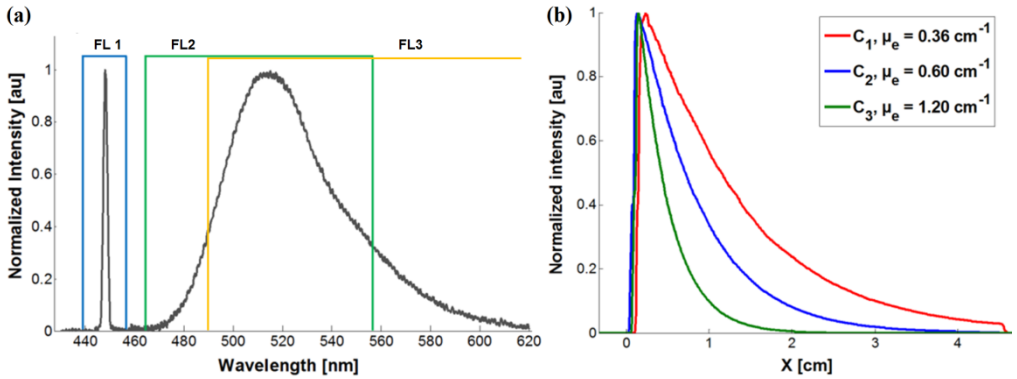

Fig. 2. (a): Emission spectra from yellow fluorescing highlighter's ink excited at 448 nm. The LIF signal is peaking at 517 nm. The Mie and LIF signals are filtered prior to detection, using two high-performance optical filters, FL1 and FL2 respectively. (b): Intensity decay of the laser sheet crossing a cuvette filled with dyed water for three different concentrations C_1, C_2 and C_3. These dye concentrations were successively tested in the spray. To avoid unwanted reflections effects from the cuvette walls, SLIPI LIF is performed here.

filter (GG495 Yellow Schott Optical Filters) together with two high-performance optical filters (95% in transmission and optical density >6 in blocking). The spectral emission of the dye can be seen in Fig. 2(a) together with the filters range. The long-pass filter is characterized by a cut-on wavelength at 495 nm and reflects most of the 448 nm incident light. The band-pass filter used for the detection of the fluorescence signal is centered at 510 nm with 94 nm FWHM (full width at half maximum). For the Mie signal, a narrow-band filter centered at 448 nm with 20 nm FWHM is used .The LIF and Mie signals are simultaneously recorded using two identical cameras positioned orthogonal to each other and at 90° from the illuminated plane (see Fig. 1). These cameras are 14-bit electron multiplying CCD cameras (Luca R from Andor), providing images of 1004×1002 pixels. A pixel-to-pixel overlapping of the images is important before processing the intensity ratio. To achieve this, the positioning and the focusing of the cameras must be carefully adjusted and the recorded images must be warped to reach a nearly equal field of view on a pixel scale. Here, the two signals are recorded with an exposure time of 0.88 seconds and 75 images are accumulated. The laser power of the modulated light sheet is reduced down to 5% of the 900 mW initial output power mostly due to light losses induced by the grating and the spatial filter (see Fig. 1). In this work, the effect of the incident light intensity on the SMD distribution is studied by adjusting the initial output laser power to P_1 = 200 mW, P_2 = 500 mW and P_3 = 800 mW. Also the effect of dye concentration on the measurement is investigated for three concentrations (C_1, C_2 and C_3) corresponding to an extinction coefficient of μ_e = 0.36 cm^{-1}, μ_e = 0.60 cm^{-1} and μ_e = 1.20 cm^{-1} respectively as shown in Fig. 2(b). Note that these extinction coefficient measurements were performed by recording SLIPI-LIF images of a cuvette containing the dyed water solution and using the Beer-Lambert law.

3.2 PDI set-up

A PDI system (PDI-200 MD) from Artium Technologies is used to calibrate the SLIPI LIF/Mie measurement (see top-view in Fig. 1). The transmitter module contains two Nd:YAG diode pumped solid state lasers (of wavelengths λ = 532 nm and λ = 473 nm). A transmitter lens of 1000 mm focal length is used to focus two 532 nm beams in the vertical and two 473 nm beams in the horizontal direction. The crossing of the four beams corresponds to the measurement probe volume which is in the order of a few hundred cubic microns. The light scattered from the droplets crossing the measurement region is collected by a receiver lens of 500 mm focal length at an off-axis angle of 36° from the transmitted beam direction. The PDI probe volume is perfectly overlapping with the modulated laser sheet in order to calibrate the

#204922 - $15.00 USD Received 16 Jan 2014; revised 12 Feb 2014; accepted 13 Feb 2014; published 19 Feb 2014

LIF/Mie images. To allocate, at a pixel level accuracy, the position of the PDI probe volume on the LIF/Mie images, the crossing point of the four beams has been imaged with the EM-CCD cameras. The spray is moved along the direction of the laser sheet (from the edge of the spray towards its center) to acquire data for every millimeter successive distribution histograms of the droplet size. For each collection point, 50 000 validated size measurements are recorded and the corresponding absolute SMD is calculated. To ensure the sphericity of the measured droplets, a 15% diameter difference threshold is set. It is observed in all measurements that the diameter validation percentage was above 96%, demonstrating good sphericity of the droplets at distance 3.5 cm below the nozzle tip.

3.3 SLIPI transmission measurements

SLIPI transmission measurements are performed in order to deduce the optical thickness of the spray. The schematic of the set-up is given in Fig. 3(a). The SLIPI-LIF signal is recorded from a glass cuvette filled with the dyed water solution (in the exact same way than for the results presented in Fig. 2(b)). The incident and final intensity profile of the laser sheet are acquired while keeping the spray "off" and "on", respectively. These profiles are shown in Fig. 3(b). The resultant spray transmission and optical depth (OD) is deduced from the Beer-Lambert law, as shown in Fig. 3(c). It is observed that only 35-40% of the incident light remains after crossing the spray, corresponding to OD~1. From this measurement it is evident that the hollow-cone spray used in this study is dilute, as most of the photons have interacted only once with the droplets prior to exit the spray system. Also noticeable is a sudden increase in OD, interpreted as the border between the spray region and the spray formation region (which is indicated with dashed box in Fig. 5).

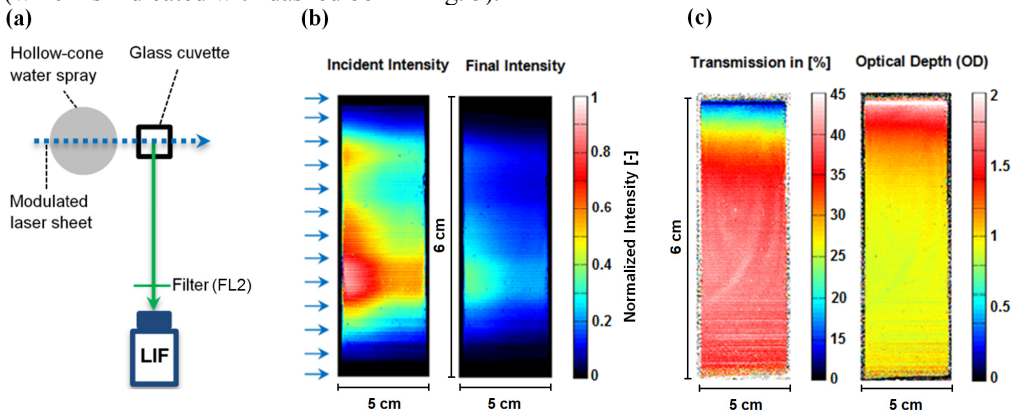

Fig. 3. (a): Top-view of the SLIPI-transmission setup is shown. (b): Incident and final intensity profiles of the laser sheet on a glass cuvette filled with dyed water solution. From these measurements the light transmission and the optical depth of the spray can be deduced along the vertical axis of the laser sheet as shown in (c). In this case, the OD is mostly close to ~1, confirming that the probed spray is dilute. Note that the vertical and horizontal dimension aspects are not equal on these images.

4. Non-calibrated results

4.1 LIF & Mie images

Three modulated sub-images of the LIF and the Mie signals are shown in Fig. 4(a). These images are recorded using the optical setup depicted in Fig. 1. The modulated light sheet is entering the spray from left side and traverses it along its central axis. A spatial phase difference of 120° between the set of two successive images is achieved by physically shifting the grating along the vertical direction. This is operated by means of a high-precision piezo actuator from Physik Instrumente. Based on these three modulated sub-images, the final conventional and SLIPI images, shown in Fig. 4(b), are extracted using Eq. (3) and Eq. (2)

#204922 - $15.00 USD Received 16 Jan 2014; revised 12 Feb 2014; accepted 13 Feb 2014; published 19 Feb 2014

respectively. The image differences between the two detection schemes are apparent. In comparison to the conventional image, the SLIPI image is "cleaned up" from undesired effects such as blurring and detection of light intensities from non-illuminated areas. A detail description of the image improvements using the SLIPI technique can be found in [25], also for the case of a hollow-cone spray. Apart of the injector design, the main difference between the two studies is the lower injection pressure used here (20 bars instead of 50 bars), making the spray optically dilute. As a result, the laser extinction effect is not clearly apparent and one can observe from Fig. 4(b) that the amount of light intensity from the entrance and exit

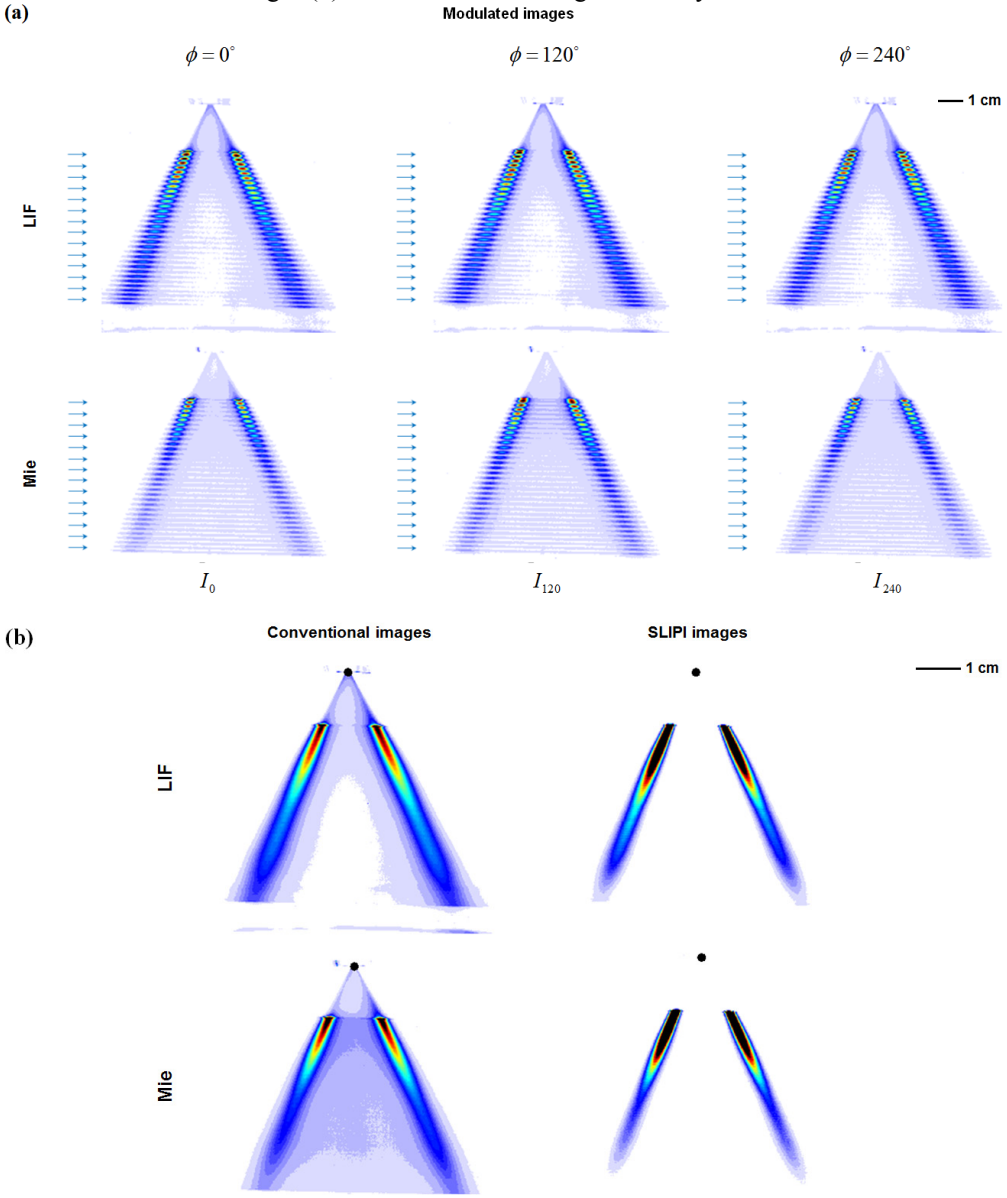

Fig. 4. The conventional and SLIPI, LIF and Mie averaged images of the hollow-cone spray are generated by recording three modulated sub-images of both signals as shown in Fig. 4(a). These modulated images are recorded with a phase difference of 120°. The conventional images, created by averaging the three modulated sub-images, and the SLIPI images, generated by taking the root-mean square of the same images, are shown in Fig. 4(b).

#204922 - $15.00 USD Received 16 Jan 2014; revised 12 Feb 2014; accepted 13 Feb 2014; published 19 Feb 2014

side of the spray remains comparable. This observation indicates that the spray is not optically dense, as verified from the transmission measurements previously shown.

4.2 Relative SMD mapping

The relative SMD distribution of droplets is shown in Fig. 5. These images are extracted from the ratio of the LIF and Mie images given in Fig. 4(b). In order to adequately compare the conventional and the SLIPI results, the images are post-processed according to the same process: The image background is first calculated from the average of 100 pixels located at the top left corner of each image. After background subtraction, a threshold value equal to 0.001% of the maximum peak intensity of the image is calculated. Any pixel value below this threshold is disregarded to avoid numerical errors while ratioing the data. It is worth mentioning here that a nearly identical SLIPI SMD image can be obtained without background subtraction. However, the same image processing routine was kept on both detection schemes for fair comparison. Several noticeable differences between the conventional, Fig. 5(a), and SLIPI, Fig. 5(b), LIF/Mie ratios can be pointed out: First, a SMD value is seen up to the nozzle tip on the conventional LIF/Mie image while this is not observable for the SLIPI case. As this part of the spray is not illuminated by the laser sheet, the corresponding SMD is extracted from multiply scattered photons only and has, consequently, no real meaning. Second, according to the SLIPI results large droplets are located on the edge of the spray while small droplets are measured at this same location with conventional planar imaging. Finally, due to global blurring effect, the spray cone does not appear as hollow for the conventional as it does for the SLIPI image.

As a result, Fig. 5(b) seems to be a convincing representation of the relative droplets SMD in opposition to Fig. 5(a). This observation needs now to be proven by the means of an additional technique where the absolute SMD can be measured. To reach this goal, the latest PDI setup from Artium Technologies has been used. It should also be noted from Fig. 5(b) that the SMD data cannot be considered near the nozzle exit (indicated on the SLIPI LIF/Mie image by the dashed rectangular area) due the presence of non-spherical droplets and ligaments. The data shown here correspond to a given dye concentration and laser power. The influence of these two parameters is investigated in the next sub-section.

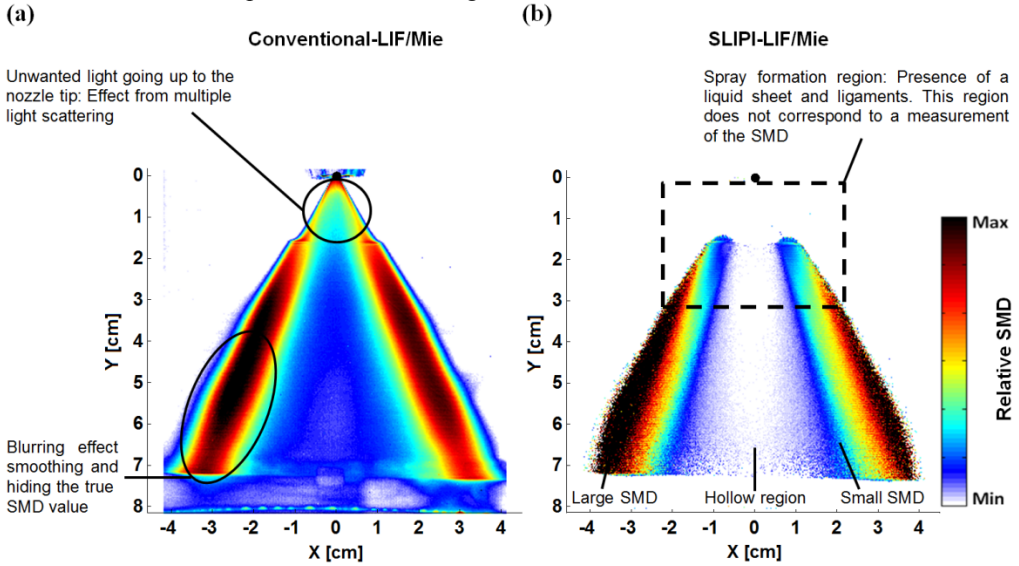

Fig. 5. Averaged images of the Conventional LIF/Mie and SLIPI LIF/Mie, in (a) and (b) respectively, representing the relative SMD of droplets distribution. Effects from the multiple light scattering are apparent on the conventional SMD image. By efficiently removing the intensity contribution from multiple light scattering those effects are suppressed, leading to a reliable SMD mapping of the hollow-cone spray as shown in (b).

#204922 - $15.00 USD Received 16 Jan 2014; revised 12 Feb 2014; accepted 13 Feb 2014; published 19 Feb 2014

4.3 Effect of dye concentration and laser power

The effect of the dye concentration, C, on the relative SMD is shown for conventional and SLIPI detection in Fig. 6(a) and Fig. 6(b) respectively. Three concentrations corresponding to C_1 (μ_e = 0.36 cm^{-1}), C_2 (μ_e = 0.60 cm^{-1}) and C_3 (μ_e = 1.20 cm^{-1}) are investigated while the laser output power is kept constant to 900 mW. In this situation the Mie scattering cross-section of the droplets should reduce in favor to the absorption cross-section due to the increase of dye molecules. However, the amount of dye was not large enough to significantly reduce the scattering cross-section and the Mie signal was observed to be nearly constant for each case of study. On the LIF detection side, the signal was naturally increased with an increase of C. As a result, the LIF/Mie ratio is showing an increase of the relative SMD value while increasing the number density of the dye molecules. The results show that the background noise decreases as C (and thereby the LIF signal) increases while the relative SMD distribution remains nearly identical. In addition, the non-linearity effects due too high dye concentration [16,17] are not observed here.

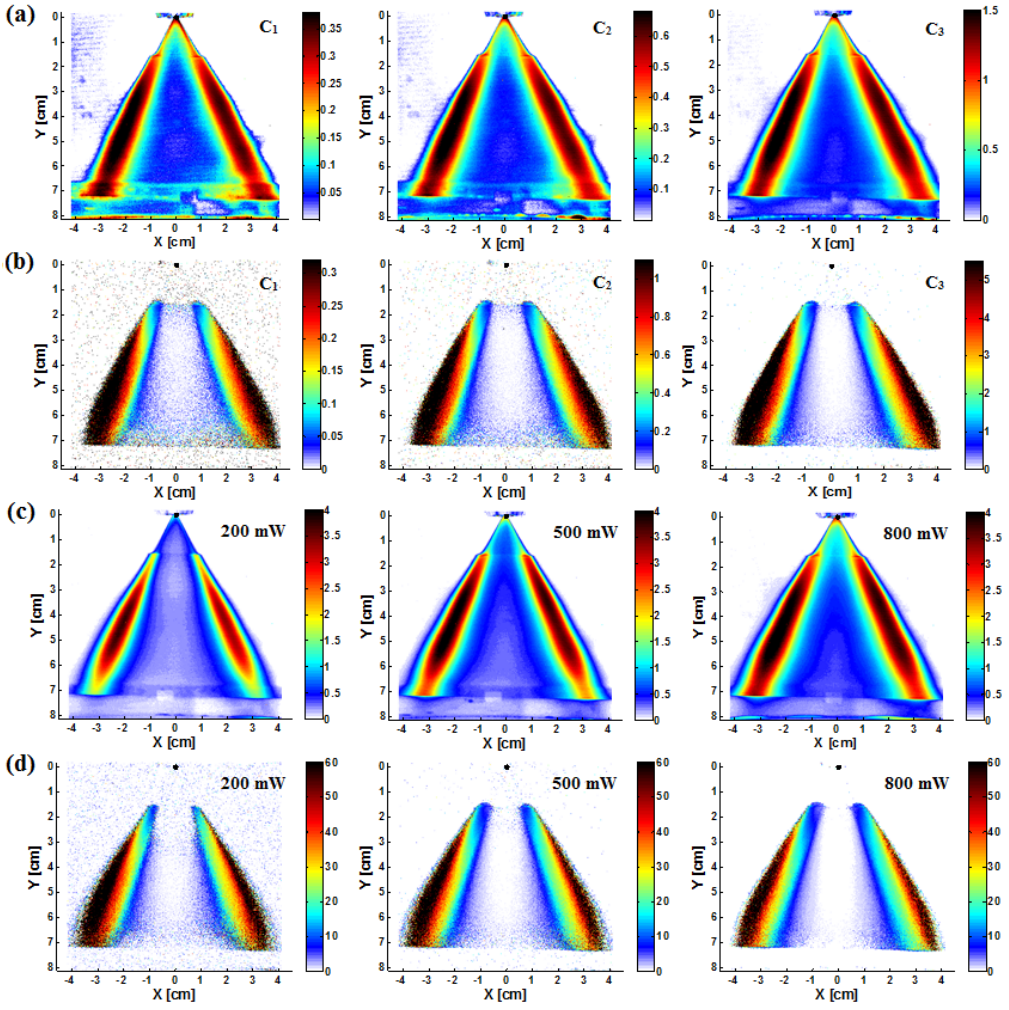

Fig. 6. Effect of dye concentration and laser power on the relative SMD distributions. Figures 6(a) and 6(b) show the conventional and SLIPI LIF/Mie ratios respectively, for the dye concentrations C_1 (μ_e = 0.36 cm^{-1}), C_2 (μ_e = 0.60 cm^{-1}) and C_3 (μ_e = 1.20 cm^{-1}). Figures 6(c) and 6(d) show the conventional and SLIPI LIF/Mie ratio respectively, at laser power P_1 = 200 mW, P_2 = 500 mW and P_3 = 800 mW.

#204922 - $15.00 USD Received 16 Jan 2014; revised 12 Feb 2014; accepted 13 Feb 2014; published 19 Feb 2014

The effect of the incident laser power, P, on the relative SMD is shown for conventional and SLIPI detection in Fig. 6(c) and Fig. 6(d) respectively. Three initial laser power corresponding to P_1 = 200 mW, P_2 = 500 mW and P_3 = 800 mW are investigated while the dye concentration is kept constant. In this situation a linear increase of P is increasing both the LIF and the Mie signals linearly resulting to a nearly unaffected SMD value. Note that in this experiment the maximum light intensity (P = 900 mW) is not sufficient to induce saturation in the dye molecules, supporting this choice for obtaining the highest SNR.

5. Calibrated results

5.1 PDI measurements

The measurement of the absolute droplets SMD using PDI is shown in Fig. 7(a). This is performed at a given vertical position (y = 3.5 cm) from the nozzle tip and along the x-axis, from one edge of the spray (at x = –3 cm) towards its center (up to x = 0.5 cm). Large droplets, SMD ~27 µm, are detected on the spray edge, while small droplets, SMD ~5 µm, are located in the spray center. This support the trend observed in the previous section for the non-calibrated SLIPI LIF/Mie results. In addition, it shows that the central part of the spray is not fully hollow and that small droplets are transported in this region due to vortical air flows.

The spacing between each data point equals one millimeter. For each of the point a droplet size distribution corresponding to 50000 droplets validated by the PDI system is considered. One example of distribution is given in Fig. 7(b) corresponding to the position x = –2.5 cm (red dot from Fig. 7(a)). In this example, a bimodal distribution can be observed where the resulting SMD equals 28.4 µm.

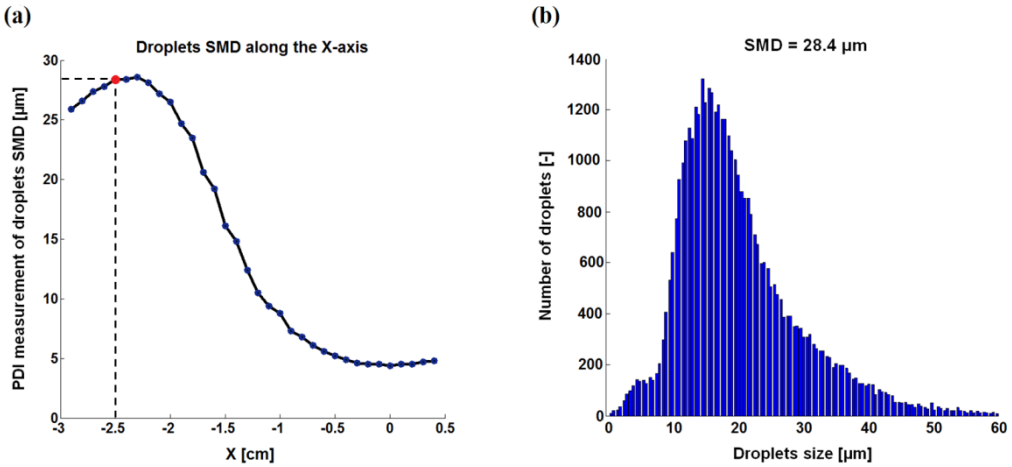

Fig. 7. Droplet size measurement using PDI. (a) Droplets SMD along the x-axis from one edge of the spray (set as –3 cm) towards its center (0 cm). The SMD is calculated from the droplet size distribution measured for every millimeter. An example of such distribution at position x = 2.5 cm (as indicated by the red dot in the Fig. 7(a)) is given in (b) where the resulting SMD = 28.4 µm.

5.2 Calibration

The SMD data from Fig. 7(a) is now used in an attempt to calibrate the LIF/Mie intensity ratios. An image of the PDI probe volume is recorded with the cameras, to deduce the exact location of the pixels that have to be considered in the calibration. For each PDI measurement point, a value of the LIF/Mie ratio is assigned as shown in Fig. 8. For the case of conventional detection, corresponding to Fig. 8(a), it is observed that for an identical LIF/Mie ratio two different SMD values are measured with PDI. For example, 10 µm and 28 µm droplets SMD are found for an identical LIF/Mie ratio equal to ~1 at different locations in the spray. This reveals that the LIF/Mie ratio cannot, in this case, be calibrated. It is, however, important to

#204922 - $15.00 USD Received 16 Jan 2014; revised 12 Feb 2014; accepted 13 Feb 2014; published 19 Feb 2014

note that the intensity contribution from multiply scattered light is very difficult to predict and the observed trend may change with the collection angle, optical turbidity, droplets size, ditribution of the droplets in the spray, *etc.* As the spray investigated here is optically dilute, this observation leads to the questioning of the accuracy of any SMD measurement when using conventional LIF/Mie in sprays. On the contrary, for the SLIPI case, corresponding to Fig. 8(a), a single solution of SMD is found for any LIF/Mie ratio. A calibration curve can be deduced allowing the relative SMD data shown in Fig. 5(b) to now be calibrated.

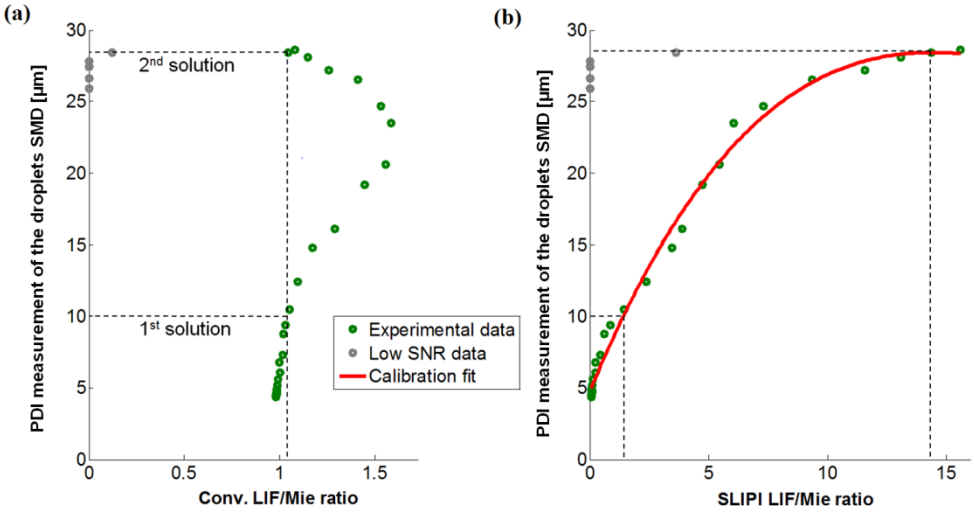

Fig. 8. Plots of the SMD values measured with PDI against the corresponding LIF/Mie ratio. In (a) the conventional case shows two SMD solutions for a single LIF/Mie ratio. In this case, the measurement cannot be calibrated. In (b) the SLIPI case shows a unique solution for each LIF/Mie ratio. This confirms the possibility of extracting a reliable calibration curve that can be used to deduce the absolute droplets SMD from Fig. 5(b).

5.3 Absolute SMD mapping

A two-dimensional map of the absolute droplets SMD is shown in Fig. 9, after calibration of the SLIPI LIF/Mie results using the red curve from Fig. 8(b).

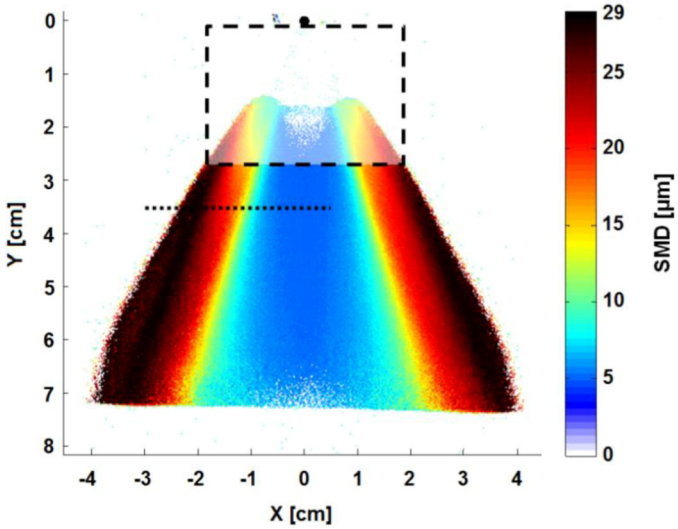

Fig. 9. Two-dimensional map of the absolute droplets SMD for a indicated on hollow-cone water spray running at 20 bars injection pressure. The result is obtained from SLIPI LIF/Mie after calibration with PDI data. The PDI measurements were performed at 3.5 cm below the nozzle tip, along the black dot line the image.

#204922 - $15.00 USD Received 16 Jan 2014; revised 12 Feb 2014; accepted 13 Feb 2014; published 19 Feb 2014

The indicated box, corresponds to the spray formation region where non-spherical droplets and ligaments are present. Similarly to the results found with PDI, the presented image shows the presence of 5 µm droplets in the central region of the spray. However, the injected water disintegrates into large droplets of ~29 µm along the spray edges which is also in accordance with the PDI measurements. Such results are unique as they cannot be obtained using conventional planar imaging where the calibration procedure is, in this case, unfeasible.

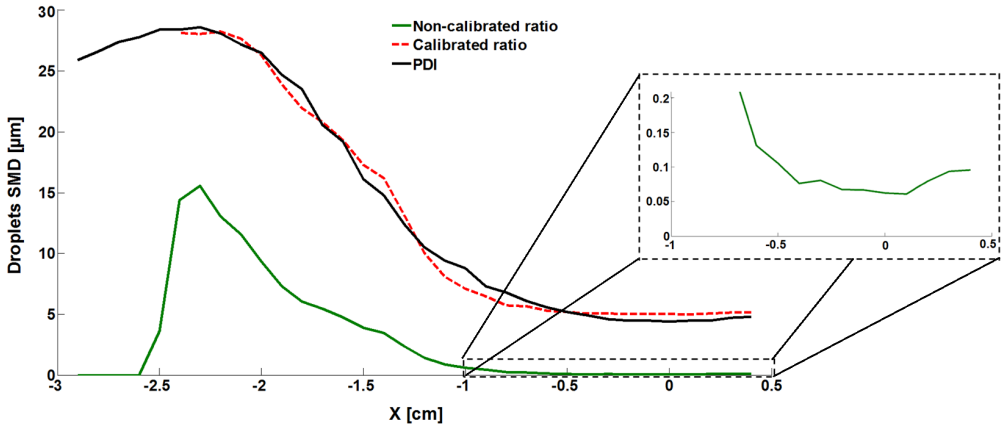

Fig. 10. Comparison of the PDI results with both the non-calibrated and the calibrated SLIPI data. A magnification of the non-calibrated ratio data between −1 cm and 0.5 cm shows that the SLIPI ratio remains non-zero in this region.

The comparison of PDI measurement with the calibrated and non-calibrated SLIPI ratios is shown in Fig. 10. It is observed that the calibrated SLIPI SMD values agree well with most of the PDI data curve, except at the edge of the spray at $x < -2.5$ cm. In this location, fewer droplets are present, inducing a low SNR on LIF and Mie signals detected by the cameras. The PDI system, which has a larger dynamic range than the EM-CCD cameras, is still capable of detecting the presence of large droplets in these regions, despite their very low number density.

6. Conclusions

In this work, it is deduced that an appropriate calibration process is not possible when using conventional PDS in a spray system, since two SMD values were assigned for a single LIF/Mie ratio value. This observation is quite surprising, as the investigated spray was not defined as “optically dense”. When using SLIPI a calibration curve was, however, possible to obtain. The trend of the SLIPI LIF/Mie results did show good agreements with the data from the PDI measurements. As a result, a reliable two-dimensional distribution of droplets SMD was obtained in a hollow-cone water spray. The investigation performed in this article strongly supports the application of the SLIPI technique for reliable droplet sizing, even for the case of optically dilute sprays. Future work will focus on the applicability of the presented calibrated approach in optically denser sprays. The presented results open up new possibilities for faithful droplet size mapping in sprays and questions, at the same time, about the reliability of the experimental LIF/Mie data presented over the past two decades.

Acknowledgments

The authors would like to thank Dr. W. Bachalo from Artium Technologies Inc. and Dr. H. Voges from LaVision GmbH for loaning the PDI system. We gratefully acknowledge the Swedish Research Council for the financial support of the Project 2011-4272. Funding from the European Research Council Advanced Grant DALDECS is also highly appreciated.

#204922 - $15.00 USD Received 16 Jan 2014; revised 12 Feb 2014; accepted 13 Feb 2014; published 19 Feb 2014